Atmos. Chem. Phys. Discuss., 13, 9801–9847, 2013
www.atmos-chem-phys-discuss.net/13/9801/2013/
doi:10.5194/acpd-13-9801-2013

Atmospheric Chemistry and Physics Discussions

Size resolved airborne particulate polysaccharides in summer high Arctic

C. Leck[1], **Q. Gao**[1,*], **F. Mashayekhy Rad**[1,2], **and U. Nilsson**[2]

[1]Department of Meteorology, Stockholm University, 106 91 Stockholm, Sweden
[2]Department of Analytical Chemistry, Stockholm University, 106 91 Stockholm, Sweden
[*]now at: Department of Chemistry, Umeå Universitet, 901 87 Umeå, Sweden

Received: 20 March 2013 – Accepted: 30 March 2013 – Published: 15 April 2013

Correspondence to: C. Leck (lina@misu.su.se)

Published by Copernicus Publications on behalf of the European Geosciences Union.

Abstract

Size-resolved aerosol samples for subsequent determination of polysaccharides (monosaccharides in combined form) were collected in air over the central Arctic Ocean during the biologically most active period between the late summer melt season and into the transition to autumn freeze-up. The analysis was carried out using liquid chromatography coupled with highly selective and sensitive tandem mass spectrometry. Polysaccharides were detected in all sizes ranging from 0.035 to 10 µm in diameter with distinct features of heteropolysaccharides, enriched in xylose, glucose + mannose as well as a substantial fraction of deoxysugars. Polysaccharides containing deoxysugars showed a bimodal structure with about 60 % of their mass found in the Aitken mode over the pack ice area. Pentose (xylose) and hexose (glucose + mannose) showed a weaker bimodal character and were largely found in the coarse mode in addition to a minor fraction apportioned in the sub-micrometer size range. The concentration of total hydrolysable neutral sugars (THNS) in the samples collected varied over 3 orders of magnitude (1 to 692 pmol m^{-3}) in the super-micrometer size fraction and to a lesser extent in sub-micrometer particles (4 to 88 pmol m^{-3}). Lowest THNS concentrations were observed in air masses that had spent more than 5 days over the pack ice. Within the pack ice area, about 53 % (by mass) of the total mass of polysaccharides were found in sub-micrometer particles. The relative abundance of sub-micrometer polysaccharides was closely related to the length of time that the air mass spent over pack ice, with highest fraction (> 90 %) observed for > 7 days of advection. The ambient aerosol particles collected onboard ship showed similar monosaccharide composition, compared to particles generated experimentally in situ at the open lead site. This supports the existence of a primary source of particulate polysaccharides from open leads by bubble bursting at the air-sea interface. We speculate that the presence of biogenic polysaccharides, due to their surface active and hygroscopic nature, could play a potential role as cloud condensation nuclei in the pristine high Arctic.

ACPD
13, 9801–9847, 2013

1 Introduction

Clouds remain a weakness in our understanding of the climate system and consequently in climate modeling (IPCC, 2007). This is especially true for Arctic low-level clouds (Walsh et al., 2002; Tjernström et al., 2008; Karlsson and Svensson, 2011). In contrast to similar clouds in mid-latitude and/or subtropical air, known to cool the climate system, Arctic low-level clouds warm the surface most of the time (Intrieri et al., 2002; Sedlar et al., 2010; Tjernström, 2005). This warming is due to an intricate balance between the optical properties of the clouds and the reflectivity of the ice cover. The optical cloud properties, in turn, are controlled of by that part of the aerosol capable of acting as cloud condensation nuclei (CCN) and ice forming nuclei. During large parts of the year the surface reflectivity is as high, or higher than the cloud albedo. During the most intense summer ice melt, the surface reflectivity is reduced, by the opening up of open-water and by formation of melt ponds on the ice. The low-lewel clouds may then become a cooling factor for a short time period. To be able to explain the maintenance of the high Arctic CCN is apparently thus a critical element in improving our ability to assess the potential role of Arctic low-level clouds on the melting and freezing of the perennial sea ice.

Recent unique results confirm for the first time that polymer gels in airborne aerosols and in clouds originated from the water (Orellana et al., 2011) and strongly support the previously unverified hypothesis of a link between cloud formation and polymer gels in the surface microlayer (SML, $< 1000\,\mu m$ thick at the air-sea interface) of the high Arctic open leads (Bigg et al., 2004; Leck and Bigg, 1999, 2005b, 2010; Leck et al., 2002; Bigg and Leck, 2008). Polymer gels, also referred to as marine colloidal gels, are produced by phytoplankton and sea ice algae biological secretions and are highly surface-active and highly hydrated (99 % water) polysaccharide molecules. These molecules are spontaneously forming three-dimensional networks inter bridged with divalent ions (Ca^{2+}/Mg^{2+}), to which other organic compounds, such as proteins

ACPD
13, 9801–9847, 2013

and lipids, are readily bound (Decho, 1990; Chin et al., 1998; Zhou et al., 1998; Verdugo, 2012 gives a review).

Blanchard (1971) and Blanchard and Syzdek (1988) have long advocated that a significant proportion of the remote oceanic aerosol is derived from two distinct processes when bubbles on seawater burst. One is from fragments of the bubble membrane (film) that are thrown into the air when the bubble bursts ("film drops"). The other is from drops of water that are detached from an upward- moving jet of water that follows the bubble burst ("jet drops"). Most commonly, the bubbles result from entrainment of air induced by wind stress at the air-water interface, which produces primary aerosol particles in CCN sizes. In this process, bubbles scavenge sea-salt, debris and high molecular weight soluble organic surface-active compounds as they rise through the water prior to their injection into the atmosphere. It has generally been assumed that particles derived from film drops would be composed of sea salt and can thus contribute a significant fraction of the CCN population (O'Dowd et al., 1999). Over the summer pack ice near surface wind speeds are typically low ($<\sim 6\,m\,s^{-1}$), and the extent of open water in leads in the pack ice is usually modest (10–30 %) so that fetches are short and the generation of waves is limited. In spite of the low winds a recent study confirmed both the presence and temporal variability of a population of bubbles within the open leads, and a non-wave bubble source mechanism, subsequently generating both film -and jet drops, driven by the surface heat flux was proposed (Norris et al., 2011). However, transmission electron microscope (TEM) studies of individual particles by Bigg and Leck (2001, 2008); Leck et al. (2002); Leck and Bigg (2005a,b) over the perennial ice have failed to find evidence of sea salt particles of less than 200 nm in diameter. To explain this, the same authors proposed a bubble-induced mechanism responsible for transporting polymer microgel rich organic material from the bulk seawater into the open lead SML. It was suggested that the highly surface-active polymer gels could attach readily to the surface of rising bubbles and self-collide to form larger aggregates. Consequently, polymer gels and their aggregate production, as well as the embedded solid particles such as bacteria, phytoplankton and its detritus can be

ACPD
13, 9801–9847, 2013

carried selectively to the surface microlayer by rising bubbles. Before bursting, bubbles rest in the microlayer and therefore are likely to have walls composed largely of gels that give them strength, with embedded particulate matter that may be points of weakness as the water drains from between the walls. Following the burst, the film drop fragments would not be drops of salt water but of surfactant material with salt-free water and any particles attached to the fragments.

Even the ability of jet drop particles that are mainly composed of sea salt to act as cloud condensation nuclei is not straightforward (Leck et al., 2002). Their observed coating of highly surface-active polymer gels over the Arctic pack ice area will most likely revert to short chain compounds after exposure to ultraviolet light (Orellana et al., 2011). Their initial highly surface-active properties may soon be reduced when airborne.

The recently demonstrated presence of the polymeric gels of open lead origin in the high Arctic airborne aerosol particles and cloud droplets was novel and based on immunological techniques (Orellana et al., 2011). The combined value of using electron microscopy detection of both single particles composed of surface-active organic gel material, bacteria in the absence of sea salt as well as sea salt particles associated with the same surface-active gel material, has clearly been shown in airborne samples collected in the pristine high Arctic summer and at remote marine locations at lower latitudes (Bigg, 1980, 2007; Gras and Ayers, 1983; Posfai et al., 2003; Leck and Bigg, 2008). Based on the technique of nuclear magnetic resonance spectra, Fourier transform infrared spectra, X-ray spectromicroscopy and Alcian blue staining (Kuznetsova et al., 2005) a few more studies at lower latitudes have shown that the chemical nature of the organic constitutes in marine aerosol particles resembles the biogenic organics containing polysaccharides from seawater. The former studies were performed at Barrow, USA (71° N, 156° W) and in the Arctic Ocean south of the ice (Hawkins and Russel, 2010, Russell et al., 2010), in the North Atlantic Ocean (Facchini et al., 2008), as well as in the southeast Pacific (Hawkins and Russell, 2010).

ACPD
13, 9801–9847, 2013

Whereas these methods have proven very useful for the understanding of the multi-component and multi-phase nature of ocean-derived aerosol particles, they are not completely quantitative (the immunological technique excluded) and obtaining statistics of the proportion of particles having a particular property promoting cloud-nucleating abilities is very time-consuming. To further strengthen the quantitative information of the contribution of polysaccharides and their monomers to the marine aerosol, necessitates size-segregated mass detection. This is further challenged in the high Arctic summer by the observed very low total airborne suspended particulate matter (less than 10 µm diameter) with median concentrations of 0.9 µg m^{-3} (Leck and Persson, 1996a).

This paper will reveal unique chemical fingerprints of airborne size-resolved polysaccharides (combined monosaccharides). The analyses have been performed with liquid chromatography coupled with highly selective and sensitive tandem mass spectrometry (LC/MS/MS). We report on measurements from the open waters along the ice edge and from within the perennial pack ice of the central Arctic Ocean during the biologically most active period between the late summer melt season and into the transition to autumn freeze-up. The ultimate aim is to provide information relevant to the CCN control of albedo of the common low-level clouds in the region and its influence on the melting and freezing of the perennial sea ice.

2 Study area and experimental approach

2.1 Location

Determinations of polysaccharides (combined monosaccharides) in airborne aerosols were performed as part of the activities of the research programs on the Arctic Summer Cloud and Ocean Study (ASCOS) onboard the Swedish icebreaker *Oden* in 2008. The interdisciplinary program was conducted in the fields of marine biology and chemistry, atmospheric chemistry, oceanography and meteorology with the overall aim to

ACPD
13, 9801–9847, 2013

improve our understanding of low-level cloud formation and possible climate feedback processes over the central Arctic Ocean.

The expedition departed from Longyearbyen, Svalbard on the 2 August 2008 (Day Of Year, DOY, 215), and headed north for the pack ice of the central Arctic Ocean. Measurements commenced on the 12 August (DOY 225) when *Oden* was anchored to a large ice-floe (referred to as the Pack Ice, PI, -drift), slightly north of 87° N (87,4° N; 1.5° W), and proceeded to drift with the ice floe for the following three weeks, until midnight between the 1 and 2 September (DOY 245–246) (87.1° N; 12° W) to return southwards. On the way to the large ice floe additional brief stations were set up: an open water station (OW1) in the Greenland Sea on the 3 August 2008 0:00 to 12:00 (DOY 216–216.5) (78.2° N; 7.5° E) followed by a 24 h station in the marginal ice zone (MIZ1) starting on the 4 August 2008 12:00 (DOY 217.5) (79.9° N; 6.1° E). On the way back, a second marginal ice edge station (MIZ2) was set up at the ice edge on the 6 September 2008 09:00 to the 7 September 2008 04:00 (DOY 250.4–251.2) (80.7° N; 8.9° E) immediately followed by a final 12 h open water station (OW2) ending on the 7 September 2008 16:00 (DOY 251.7) (80.4° N; 10.1° E) in the Greenland Sea before arriving at Longyearbyen on 9 September (DOY 253). A map of the route with the ice drift magnified is shown in Fig. 1. All times are reported in Universal Time Coordinate (UTC). For further cruise details see Paatero et al. (2009) and Tjernström et al. (2013).

2.2 Atmospheric sampling of aerosol particles onboard ship

In order to optimize the distance both from the sea and from the ship's superstructure the sampling inlet for airborne aerosol particles extended at an angle of 45° to about three meters above the container roof on the 4th deck, 23 m above sea level. An Andersen impactor (Anderson Inc., Atlanta, Ga) at the top of the sampling line excluded particles $D_p > 10\,\mu m$ (PM_{10}) in equivalent aerodynamic diameter (EAD) at ambient relative humidity. The total flow through the 9 cm inner diameter sampling line pipe was about 1000 $L\,min^{-1}$, which resulted in a residence time of < 1.4 s and a Reynolds number of 21 000. The turbulent flow in the main inlet ensured that the air was well-mixed

ACPD
13, 9801–9847, 2013

when sampled by the isokinetic secondary lines connected to the sampling impactors in use. The impactor intakes were controlled to maintain 50 % relative humidity. The PM_{10} inlet was identical to the one used during three previous expeditions to the same area and time of year (Leck et al., 1996, 2001, 2004) and details on its position and design on board the *Oden* are further described in Leck et al. (2001).

To maximize the sampling time it was required that the mast was facing upwind. During the PI-drift this necessitated a "harbor" in the ice in which the ship could be moored in several different directions and turned as the wind direction changed. In addition direct contamination from the ship was excluded by using a pollution controller, turning off all the pumps of the sampler, in direct connection to the sampling manifold. It consisted of a TSI-3025 counter connected to the control system described by Ogren and Heintzenberg (1990). The quality of the samples was additionally monitored using various combustion tracers and wind speed – and direction thresholds: provided that the wind was within ±70° of the direction of the bow and stronger than 2 m s^{-1}, no ship pollution reached the sample inlets. Fur further details see Leck et al. (2001).

Low pressure Berner Cascade Impactors (BCI) (Berner et al., 1979) were used to collect samples for determination of the monosaccharides. The flow rate of sampling was 77 L min^{-1}. The BCI collected enough material for analysis in 20 h in the early stages of the voyage but sampling times had to be increased to as long as 40 h later in the voyage. Field blank samples were obtained by setting the impactors with loaded substrates at the sampling site with the same sampling period without air passing through. In total, 18 duplicate BCI samples were collected during the course of AS-COS.

The BCI's collected particles in the size ranges < 0.161 (stage-1, back-up), 0.161–0.665 (stage-2), 0.665–2.12 (stage-3), 2.12–5.0 (stage-4), 5.0–10 (stage-5) µm, EAD (50 % collection efficiency). Converted to dry (20 % RH) geometric mean diameters, the BCI size ranges corresponded to < 0.113, 0.113–0.489, 0.489–1.58, 1.58–3.73 and 3.73–7.47 µm. In comparison with Covert et al. (1996), the BCI with five stages thus enabled detection of chemical composition in Aitken mode (lowest stage), accumulation

ACPD
13, 9801–9847, 2013

mode (stage 2) and coarse mode (stage 3–5). Millipore Fluoropore membrane filters (pore size 1.0 µm; diameter 47 mm) were used for stage-1. The Millipore filter has a 99 % collection efficiency for particles with diameters larger than 0.035 µm (Liu and Lee, 1976). Pre-cleaned Tedlar® polyvinyl fluoride films (DuPont) were used as particle impaction substrates for the other four stages. Ambient samples and blanks were carefully handled in a glove box (free from particles, sulfur dioxide and ammonia) both prior to and after sampling. All substrates for determination of organic compounds were flash-frozen in liquid nitrogen directly after unloading and stored at −80 °C until further treatment.

2.3 In situ generation of nascent aerosol by artificial bubble bursting at an open lead site

The bubbling experiments were made at a field site located at the edge of an open lead approximately 3 km from the *Oden*. The width of the open lead varied from day to day with the movement of the ice from around 20 m to 100 m. From a floating platform approximately two meters from the edge of the ice floe, filtered, particle-free air was released under water through two porous sintered glass frit (nominal pore size 15–25 µm) heads located 10–20 cm below the water surface. The bubbling source was driven by a battery-operated pump at a flow rate of 200 mL min^{-1}, which enabled that a sufficient number of gentle bubbles of about 500 µm in diameter (to represent ambient conditions at the open lead; range 30–560 µm, (Norris et al., 2011)) could be generated. Two holders were placed above the bubble bursting region at a height of 10–30 cm above the water surface. The nascent particles were collected onto pre-cleaned 1 µm nylon filters using a vacuum pump with a flow rate of 18 L min^{-1}. Collection times lasted from 30 min to 3 h.

ACPD
13, 9801–9847, 2013

2.4 Determination of monosaccharide composition

The aerosol particles collected on the substrates or filters were ultrasonically extracted with ultrapure water (Milli Q, Resistivity 18.2 MΩ cm). The samples were vacuum-dried and then hydrolyzed with 4 M trifluoroacetic acid (TFA) at 100 °C for 2 h. The hydrolysate after removal of excess TFA was reconstituted in acetonitrile and water (80 : 20, *v*/*v*). Details about the hydrolysis procedures are found in a previous work by Gao et al. (2010). Determination of the 7 target monosaccharides (*pentoses*: xylose and arabinose, *hexoses*: glucose, mannose and galactose and *deoxysugars*: rhamnose and fucose) was carried out using LC/MS/MS (TSQ Vantage, Thermo Fisher Scientific, Waltham, MA). Chromatographic separation was performed at room temperature using an aminopropyl-silica column (150 × 2.1 mm, 5 µm, ZorbaxNH_2, Agilent Technologies, Santa Clara, Ca), with a mobile phase composed of acetonitrile and water (80 : 20, *v*/*v*). The system was operated at isocratic condition with a flow rate of 400 µL min^{-1}. Injection volume was 5 µL. The LC system (Accela, Thermo Fisher Scientific) was coupled to a triple-quadrupole mass spectrometer equipped with heated electrospray ionization (ESI) interface operating in negative mode. Quantification was undertaken in selected reaction monitoring (SRM) mode with deprotonated monosaccharides as precursor ions ([M-H]$^-$, corresponding to *m/z* 179, 163 and 149) and fragment ions at *m/z* 59 and 89. The main MS conditions were as followed: ionization voltage 3.5 kV; capillary temperature 300 °C; vaporizer temperature 250 °C; collision gas pressure (Ar) 0.5 mTorr; mass resolution 0.7 Da for both the first- and third quadrupole. More information about instrumental working parameters are given by Gao et al. (2011).

The glucose and mannose peaks were not baseline separated. Instead, they were quantified as the sum of the sugars (glucose + mannose). This was considered reasonable due to their identical response factors. The RSD % values, as a measure of precision, were below 12 % and the instrumental limits of detection (LOD) were in the range 0.7–4.2 pg injected onto the column (Gao et al., 2011). All determinations were

ACPD
13, 9801–9847, 2013

corrected for blank levels and expressed in pmol m^{-3} at standard temperature and pressure (STP; 273.15 K and 1013.25 hPa). In the text to follow the sum of the individual monosaccharides, determined by hydrolysis and subsequent LC/MS/MS analysis, is referred to as total hydrolysable neutral sugars (THNS). Aerosol mass concentrations are expressed per unit of volume at standard temperature and pressure (STP; 273.15 K and 1013.2 hPa).

3 Data sets and data processing

3.1 LC/MS/MS determination

Triple-quadrupole LC/MS/MS with ESI in SRM mode, as utilized in this study, is a highly selective technique. The two filtering stages for the specific precursor-to-fragment transitions enabled substantial reduction of the sample matrix interferences, with improved LOD as a result. This is of great advantage for the determination of trace-level polysaccharides within a complex matrix including the interfering substances from collection substrates (e.g. Tedlar film or Teflon filters), the biological matrix (i.e. peptides and lipids associated with EPS) and the inorganic sea salts, which could account for a large part of the super-micrometer aerosol mass (Leck and Persson, 1996a; Leck et al., 2002). The method has been evaluated previously regarding linearity, accuracy, precision, matrix effects and LOD (Gao et al., 2011). For the application to aerosol mass determinations, the accuracy was revalidated by analyzing replicates of blank filter samples spiked with monosaccharide standards at two concentration levels (40 and 200 ng mL^{-1}) and thereafter treated in the same way as the ambient aerosol samples described above. LOD and limits of quantification (LOQ) of the analytical method (IUPAC, 1978) were defined as 3 and 10 times, respectively, the standard deviation (SD) of the results from the blank filters. LODs were shown to range from 6.4 to 12.6 ng mL^{-1}. By assuming a sampling volume of 100 m^3 of air (24 h sampling at the designated BCI flow rate of 77 L min^{-1}), the detection of monosaccharides in levels as low as

ACPD
13, 9801–9847, 2013

0.13–0.28 pmol m^{-3} would be possible. Duplicate BCI sample including the 7 target monosaccharides agreed on average within 25 %. To our knowledge this application of LC/MS/MS to the determination of natural occurring monosaccharides in airborne aerosols over a remote marine area is novel. The results of method validation are summarized in Table 1.

3.2 Air mass trajectories and time spent over the pack ice

The NOAA HYSPLIT (Hybrid Single-Particle Lagrangian Integrated Trajectory) model (Draxler and Rolph, 2011; Rohph, 2011) was used to calculate three-dimensional five and ten day back-trajectories of the air reaching *Oden's* position during the PI-drift for an arrival height of 100 m above surface level at hourly intervals. The trajectory calculations were based on data from the Global Data Assimilation System (GDAS) of the National Weather Service's National Center for Environmental Prediction (NCEP). Back-trajectories have several sources of uncertainty, which generally grows with the length of the trajectory. Most uncertain is transport in the vicinity of strong gradients, such as frontal zones while within a single air mass the trajectory calculations are likely more reliable. For the extent and distribution of the pack ice, ice maps from Satellite-sensor, AMSR-E, "level 1A" with the data sourced from NSIDC (Boulder), United States, finalized at Bremen University, http://iup.physik.uni-bremen.de:8084/amsr/amsre.html were used.

With the help of the back trajectories and ice maps the time elapsed since the air was last in contact with the open ocean was computed for ASCOS in the same way that Nilsson (1996) used. It will be referred to as days over ice (DOI). The calculated DOI thus marks the end point for an air parcel that left the ice edge between 0–10 days ago (resolved by the length of the trajectories). The measure of DOI will in the later analyses be used as a simple parameter to summarize the evolution of the aerosol particles as a function of the synoptic scale systems since their last contact with open sea. Figure 2 collects the cumulative travel times over ice for ASCOS, where all travel

ACPD
13, 9801–9847, 2013

times beyond five days are given the value five. Figure 2 shows that most trajectories spent at least three days (median 3.3 days) over the pack ice before reaching *Oden*. Travel times less than two days were encountered around 30 % and for travel times of four days and longer about 40 % of the cases were covered.

4 Conditions influencing the characteristics of the airborne colloidal gels

4.1 Long-range advection and general conditions encountered

The synoptic scale systems advecting heat, moisture, and particulate matter from the ice edge and open water in between the ice floes, for a variable length of time over the pack ice, will affect the chemical and physical transformations and hence properties of the observed particle size distributions at the location of the ship. Tjernström et al. (2012) summarize the meteorological conditions during ASCOS. From August to early September in 2008, the meteorology was characterized by high-pressure over the Canadian Basin and low-pressure over northern Norway into the Kara Sea, which generated an anticyclonic large-scale flow over much of the central Arctic Ocean. As a result, several low-pressure systems propagated westward, around the North Pole and across the path of ASCOS in the North-Atlantic sector of the Arctic, especially during the first half of the expedition (DOY217 to DOY228). After this, the synoptic-scale weather became more inactive (DOY229 to DOY243), with the formation of a high-pressure system over Svalbard, which moved slowly towards and across the North Pole and dominated the weather conditions from DOY244 almost until the end of the expedition. This gave a variety of cloud conditions including deep frontal systems with heavy snow, complex multi-layered systems, boundary layer fogs, and persistent low-level stratiform mixed-phase clouds. In all, clouds occurred more than 90 % of the time. In general conditions were consistently very moist, with relative humidities rarely under 90 % while near-surface winds were most often (70 % of the time) in the 2–6 $\mathrm{m\,s^{-1}}$

ACPD
13, 9801–9847, 2013

range and seldom $> 10\,m\,s^{-1}$ and confined to the synoptically active period in the beginning of the expedition.

The advection of air masses during the course of the PI-drift was typical for the central Arctic in summer (Fig. 3a). The air masses originated from the open seas surrounding the central Arctic dominated. In agreement with earlier high Arctic summer studies, air from either continents or subsiding from the free troposphere was of much less importance (Bigg et al., 1996, 2001; Leck and Persson, 1996a). The back-trajectories shown in Fig. 3b–e, were for the PI-drift subjectively classified in four clusters depending on their geographical origin: the origin of the air during both the 1st (DOY 227, DOY 229–232) and 2nd (DOY 228, DOY 236, 238–239) clusters was highly variable on a daily time bases as of the very synoptically active period during the first half of the expedition. The air masses of cluster 1 (Fig. 3b) originated easterly from the Barents and Kara Seas. For cluster 2 (Fig. 3c), they came from the Fram Strait-Greenland Sea area. During both clusters the air mass spent a relatively short time over the ice (DOI ~ 2) since last contact with open sea. The air mass origin during the 3rd cluster (DOY 234–235) was mainly from Greenland (Fig. 3d). The air trajectories showing a subsiding pathway from the free troposphere via across Greenland to the surface, which suggests that the air sampled onboard *Oden* was of free tropospheric origin. As in this case the trajectories did not have any contact with the open sea no DOI could be calculated. During DOY 240–246 (4th cluster, Fig. 3e) the air mass flow was largely from northwestern circumpolar over the pack ice for approximately DOI = 8 and from the direction of the Laptev and East Siberian Seas towards the end of the period but still with no close contact with open sea. During the OW1 and MIZ1 (DOY 216–218) we experienced air predominantly from the ice covered archipelago north of Canada and Alaska, whereas during MIZ2 and OW2 the air came from Kara Sea area with possible adjoining land contact.

Surface air temperatures varied substantially from near 0 to −12 °C but were observed mostly in the −2 to 0 °C interval. The colder temperatures prevailed in a brief episode and in a period appearing towards the end of August. A more detailed

ACPD
13, 9801–9847, 2013

description of the PI-drift would allow for a division into four separate regimes (R) based on the analyses of the surface energy budget (Sedlar et al., 2010): (1) (R1) DOY 226 to DOY 233 (dominated by the 1st trajectory cluster) had numerous melt ponds on the ice surface, with temperatures around 0 °C, 2) the melt was followed by the 2nd regime (R2) with a drop in temperature to −6 °C for about 2.5 days (DOY 234 to DOY 237 including the 3rd trajectory cluster), (3) the conditions in the 3rd regime (R3, DOY 240 to DOY 243, the former part of the 4th trajectory cluster, Fig. 3f) were governed by a persistent stratocumulus layer that contributed to maintain the temperatures between −2 to −3 °C, (4) the 4th regime (R4) (latter part of the 4th trajectory cluster, Fig. 3g) started on 31 August (DOY 244) and ended on 2 September (DOY 246) as the persistent stratocumulus layer went away and the clouds, if present, became optically thin (Mauritsen et al., 2010), which resulted a drastic drop in temperature to −12 °C and sunny conditions.

As reported by Sirevaag et al. (2011) water temperature, on the contrary, varied within a narrow range between −1.73 and −1.68 °C, causally related to the high concentration of ice within the pack ice area. The well mixed upper layer was about 28 m in depth with little variation in terms of both temperature and salinity. Salinity was 32 psu on average with pronounced influence of fresh water. Below the surface mixing layer was a uniform cold layer with a strong salinity gradient forming the upper cold halocline layer which extended down to around 100 m depth from where the temperature increase made the density increase smaller.

There was a transition from the “marginal ice zone” having 20–70 % ice cover and the “pack ice region” having between 80–95 % ice cover. The ice floes were up to several km in diameter, with thicknesses between 1.5 to 8 m (on average 2.5 m). The floes were interrupted by irregular patterns of meandering and ever-changing open water channels (“open leads”), ranging from a few meters up to 2000 m in width. During the course of the PI-drift the leads were completely ice free during R1 and the R3. During R2, heavy rimming and frost deposits was observed onto the surface of the now frozen ponds. At the sampling site, the lead started to freeze on DOY 233 and was covered

ACPD
13, 9801–9847, 2013

with a layer of frazil ice until DOY 238 (R3) when the lead opened up exposing open water again. The melt ponds recovered but were at times covered with a thin layer of dry snow. On DOY 245 (R4), freeze-up of surface water of the open leads was observed.

4.2 Vertical mixing

The vertical structure of the atmosphere was typical for central Arctic summer during the course of the expedition. The atmospheric boundary layer (ABL) was shallow and well-mixed with depths usually below 200 m. The ABL was capped by a temperature inversion with a stable stratification of the atmosphere aloft due to the advection of warmer air masses from the south (Tjernström et al., 2012).

In general the air sampled during the course of ASCOS was confined to a well mixed surface based layer. However during DOY 240–242 (4th trajectory cluster) our sampling coincided with the recoupling and turbulent mixing between a shallow (~ 150 m deep) surface-based mixed layer with the upper part of the boundary layer – the upper half of which contained stratocumulus clouds. This re-coupling can be clearly identified in radiosonde and turbulence profiles from a tethered balloon (M. Tjernström, personal communication, 2013). Back trajectory analysis suggests that the air in the upper boundary layer had come from the Canadian archipelago while that in the lowest 100 m had been over the ice for at least 10 days.

4.3 The biological source strength

If the characteristics of the derived gel-particles when bubbles on seawater burst could be fully understood their presence related to biological activity of the SML also needs to be specified. Within the SML, biological activity is influenced by such factors as depth of the surface mixed layer and stratification below it, ice conditions, temperature, available light and nutrient concentrations. The general oceanic circulation in turn influences all these factors (Leck and Persson, 1996b). The amount of light available for biological growth is of course very strongly seasonal in Polar Regions. During ASCOS the sun

ACPD
13, 9801–9847, 2013

was consistently above the horizon. This seasonality in avaible light is enhanced by the corresponding changes in ice cover, the formation of melt pools and the removal of dry snow in summer which greatly increase the available radiation at a given depth in the sea (English, 1961). The changes in ice conditions encountered during the ice drift are therefore likely to be very important to biological activity, influencing both available light and the depth of the SML.

While the increasing light and the formation of a stable mixed layer during melting (R1 and R3) of the pack ice, maximum in the month of August, favour phytoplankton growth the melt also releases nutrients derived from winter storage. The peak in phytoplankton biomass is reached as nutrients in the mixed layer approach exhaustion. Moreover, the ice itself is a source of phytoplankton, which can be released into the mixed layer during melting and may act as an inoculum for blooms (Smith and Nelson, 1985). According to previous high Arctic summer studies (Leck and Persson, 1996b; Olli et al., 2007), mineral nutrients including nitrate, phosphate and silicate should have been sufficiently high to support primary production during ASCOS. Also at the same location and season as ASCOS, the abundance, molecular size, chemical composition and reactivity of dissolved organic matter was in turn reported by Matrai et al. (2008) to vary considerably as a function of the level of biological activity in the SML and the underlying water (upper ca. 30 m).

In a parallel study during ASCOS (Gao et al., 2012), it was proposed that bubble scavenging of surface-active polysaccharides was one of the possible mechanisms for the enrichment of polysaccharides in the SML located at the air-sea interface. They were suggested to be brought there by diffusion, by Langmuir circulations, and by the surfaces of air bubbles rising through the water. Gao et al. (2012) also observed that newly released gel polymers from sea ice algae were more favorably scavenged into the SML, which is consistent with the idea that the porous nature of sea ice not only provides a habitat for ice algae but also opens a pathway for exchanges of organic matter with the seawater below. Thus it can be concluded that the melting sea ice containing high standing stocks of microalgae and bacteria elevates the input of polymer

ACPD
13, 9801–9847, 2013

colloidal gels into seawater and subsequently enhances the enrichment of polysaccharides in the SML at the air-sea interface. The source of polysaccharide containing aerosol particles could therefore likely be strengthened in summer when biological activity in the adjacent seawater is high. The same processes promoting the formation of SML polymer gels and their saccharides would also apply to the MIZ under melt. Based on the above-described observations, the most biologically active period during the PI-drift, at 87° N, could be concluded to span the transition period from the end of the summer melting to the onset of the autumn freezing-up whereas at the open waters along the ice edge, at ca. 80° N, summer conditions prevailed until the end of ASCOS in early September.

5 Atmospheric particulate mass concentrations of polysaccharides

5.1 Concentrations shown as total, sub- and super-micrometer size fractions

Table 2 tabulates basic descriptive statistics of all combined monosaccharides measured during the length of the expedition, August through the beginning of September. The data is shown separately for open water (OW 1,2), marginal ice zone (MIZ 1,2) and pack ice (PI-drift) measurements. The mass determinations of the 5 BCI stages were grouped to represent the sub-micrometer diameter range (sum of stage 1, 2, 0.035–0.665 µm) and the super-micrometer range (sum of stage 3, 4 and 5, 0.665–10 µm). For the samples collected during the PI-drift the 25th, 50th (median) and 75th percentile values of the relative abundance of both THNS and each of the monosaccharide were additionally calculated. Table 2 also tabulates detection frequencies for both THNS and the individual monosaccharides determined. The temporal variability of THNS in the grouped BCI data is depicted in Fig. 4.

In the Greenland Sea–Fram Strait area, concentrations of THNS summed over all BCI stages ranged from about 225 pmol m^{-3} (OW1) and 189 pmol m^{-3} (MIZ1) in August to about 129 pmol m^{-3} in (OW2) and 101 pmol m^{-3} (MIZ2) in September. For the PI-drift

ACPD
13, 9801–9847, 2013

a weak trend was observed with slightly elevated median concentrations measured for R1 and R2 (47 pmol m^{-3}) compared with R3 and R4 (25 pmol m^{-3}). R2 were relatively colder with leads starting to freeze on DOY 233, with a layer of frazil ice, until DOY 238 (R3) when the lead opened up exposing open water again for the final lead freeze-up at the end of R4. In September both the OW and MIZ concentrations of THNS had declined by about 45 %, within 6 weeks. All monosaccharides determined were lowest in concentrations in air masses that had spent more than 5 days over the pack ice area since last contact with open sea (discussed further in Sect. 6). The above results are not only consistent with the relatively more biologically active waters of the Greensand Sea–Framstrait area (Leck and Persson, 1996a,b; Gao et al., 2012) but also consistent with observations of the aerosol source strength based on the eddy-covariance flux measurements during ASCOS (Held et al., 2011a) and during a similar expedition to the same area and season during 1996 (Nilsson et al., 2001), which showed an order of magnitude stronger flux of bubble bursting aerosol particles over the open sea than from open leads.

The temporal variability in the grouped BCI data (Fig. 4) appeared in general similar in the sub- and super-micrometer particles. However, episodically a remarkable gradient in concentrations was observed during DOY 238 to 245 with a minimum on DOY 242. The THNS concentrations in the super-micrometer subset varied considerably over 3 orders of magnitude ranging from 1.1 to 692.0 pmol m^{-3}. The THNS concentrations in sub-micrometer particles exhibited less variability ranging between 4.3 to 88.3 pmol m^{-3}. For samples collected during the PI-drift a sub-micrometer to total THNS median molar ratio of 53 % was calculated. The samples collected in the Greenland Sea–Fram Strait area on the outward transit exhibited a corresponding molar ratio of 73 % for MIZ2 and 66 % for OW2, respectively, whereas those collected during OW1 and MIZ1 showed lower ratios (both 39 %). Among the 7 targeted analytes, xylose (pentos) and glucose + mannose (hexoses) were the predominant monosaccharides (detection frequency > 80 %), accounting for over 63 % (mole %) of the total mass of monosaccharides determined.

ACPD
13, 9801–9847, 2013

5.2 Mass median size distributions

From the full mass median size distribution (5-stage BCI) data, the 25th, 50th (median), and 75th percentile values of monosaccharides grouped into three categories (*pentoses*: xylose and arabinose, *hexoses*: glucose, mannose and galactose and *deoxysugars*: rhamnose and fucose) were calculated for the OW1,2 (number of samples $n = 2$), MIZ1,2 ($n = 2$) and PI-drift ($n = 14$) subsets, respectively. The result is presented in Fig. 5. The large span observed for the three subsets (OW/MIZ/PI-drift) implied that there was a high degree of spatial and temporal variability in the mass concentrations resolved over size. Also the uncertainty measure in the waters along the ice edge is probably biased as of the small numbers of samples available in Greenland Sea–Fram Strait area.

Size distributions of deoxysugars were clearly bimodal both over the pack ice and in the Greenland Sea–Fram Strait area with PI-drift: 56 ± 30 (1σ) %, MIZ: 81 ± 13 (1σ) % OW: and 91 ± 11 (1σ) %, respectively, of the mass occurring in the Aitken mode (stage 1). Close to half (43 %) of the pentose and hexose samples collected over the pack ice showed a bimodal character, but less pronounced, with peak concentrations frequently associated with the coarse mode (stage 4). Relative to the deoxysugars a larger fraction of the sub-micrometer mass was proportioned in the accumulation mode (stage 2): pentose 24 ± 25 (1σ) % and hexose 23 ± 22 (1σ) %. The corresponding numbers for the sum of the Aitken and accumulation modes (stage 1 + 2) were: pentose 46 ± 33 (1σ) % and hexose 54 ± 39 (1σ) %, respectively. Similar, with a weak bimodal character were the observed hexose size distributions in the MIZ of the Greenland Sea–Fram Strait area with 48 ± 33 (1σ) % of the mass occurring in the sum of the Aitken and accumulation modes. For pentose the maximum sub-micrometer concentration was however more distinctly associated with the smallest particles (Aitken mode) 46 ± 17 (1σ) %. For the samples collected over the Greenland Sea (OW1,2) peak mass concentrations for the pentose and hexose components were found in the largest size fractions with at least 50 ± 23 (1σ) % associated with the coarse mode (stage 3, 4 and 5). In general

ACPD
13, 9801–9847, 2013

for the samples collected over the pack ice, peak levels for coarse mode mass occurred interestingly in the middle size fraction (stage 4). This would tend to indicate a gradual removal of the jet drop sized aerosol particles sourced from the open sea and ice edge zone as the air passes over the pack ice. Nilsson and Bigg (1996) and Leck et al. (2002) observed a high frequency of stratiform cloudiness accompanied by advection fogs during transport of air from open sea to pack ice. This relatively efficient wet-removal by sedimentation combined with a weak particle source strength (Held et al., 2011a,b), causally related to the typically low winds ($< 6\,m\,s^{-1}$) and to the modest extent of open leads, could have accounted for a significant loss of large particles. To some extent this feature was also indicated in the MIZ samples collected in foggy conditions.

Deoxysugars have frequently been found in phytoplankton exudates and in non-photosynthetic microbial (i.e. bacteria) polysaccharides (Mopper et al., 1995; Zhou et al., 1998). Deoxysugars in seawater usually occur in elevated levels due to their relative slow rate of degradation relative to other sugar units of the polymer gel composition (Giroldo et al., 2003). According to other studies of seawater, the abundant glucose + mannose (hexoses) and xylose (pentos) in the samples collected could be associated with the cellular materials of phytoplankton, and thus belong to the family of structural and/or storage polysaccharides (i.e. xyloglucan, glucan or glycoprotein) (Panagiotopoulos and Sempere, 2005; Skoog and Benner, 1998). It is also possible for these sugars to be part of the major components of bioavailable polysaccharides and could thus easily degraded via microbial utilization into oligosaccharides and subsequently to monomers in free form. The hexose measured in the accumulation and coarse modes during this study could therefore not only have resulted from dissolved organic matters (mainly glucose) but also from phytoplankton exudates via the generation of film and jet drops at the air-sea interface.

ACPD
13, 9801–9847, 2013

5.3 Comparison with other studies

As this is a novel study, with first time determination of naturally occurring monosaccharides in combined form (polysaccharides) in size resolved airborne aerosols, direct comparison with other measurements is not possible. Instead an indirect comparison was obtained by two other methods. The first method compared the levels of our measured polysaccharides with reported levels of amino acids in marine airborne aerosol particles. Amino acids and carbohydrates are two major classes of biochemicals in seawater and have been shown to account for 1–3 % and 2–6 % of dissolved organic matters, respectively (Hansell and Carlson, 2002). The monomeric units of these two classes of biochemicals could thus be assumed to be present in similar magnitude in bubble generated aerosol. The levels of combined amino acids in bulk aerosol samples collected over the remote Atlantic Ocean were reported to be in the range of 20 to 400 pmol m^{-3} (Wedyan and Preston, 2008). Widell (2009) reported amino acid concentrations in the range of 13 to 89 pmol m^{-3} in airborne aerosol particles collected over the pack ice area during the same season as ASCOS. These levels are comparable to the THNS measured in this study. The second approach compared the reported levels from a parallel study during ASCOS, the determined non-refractory organics in sub-micrometer aerosol in air by Chang et al. (2011), using an aerosol mass spectrometer. The estimated fraction of the dissolved organic matter in seawater characterized as neural sugars was about 1.5–3 % (2.7 % on average) (Gao et al., 2012), which would correspond to the order of 10 pmol m^{-3} THNS based on the estimates of submicrometer organics in the study of Chang et al. (2011). This is again comparable to our results, with a measured mass concentration of THNS between 15.8 to 42.5 pmol m^{-3} (between the 25th and 75th percentiles).

ACPD
13, 9801–9847, 2013

6 Changes in polysaccharides in relation to changes in source strength, long-range advection, and vertical mixing

6.1 Changes over the four regimes

The four regimes encountered during the PI-drift is indicated if Fig. 4. Regime 1 (DOY 226 to 233) was dominated by the 1st trajectory cluster (Fig. 3b) with air masses originating easterly from the Barents and Kara Seas and a relative short time (DOI = 2 days) spent over the pack ice. Within this trajectory cluster the THNS mass concentrations of the particles collected at the position of the ship (about 87° N) were the highest and distributed approximately with 2/3 of the mass within the Aitken and accumulation modes (Fig. 6). On DOY 231 a significant enhancement of THNS was observed in the both the sub- and super-micrometer size range (Fig. 4). Calculated super-micrometer Cl^-/Na^+ molar ratios in parallel BCI samplers onboard ship (C. Leck, unpublished data), resulted in a molar ratios of ca. 1.0 (DOY 230), which showed very recent sea-salt production from jet drops (Leck et al., 2002). Even if the jet drop particles were mainly composed of sea salt, their past observed coating of highly surface-active polymer gels (Leck et al., 2002) would most likely have explained the high super-micrometer THNS concentrations observed. A similarly active film drop mode would explain the sub-micrometer enhancements. The samples collected with the 2nd trajectory cluster, depicted in Fig. 3c, (minor part of R1 and during the transition between R2 and R3) were influenced by air masses from the Greenland Sea–Fram Strait area around 2 days ago. Average THNS mass concentrations measured (Fig. 6) were about 70 % lower in the super-micrometer particles. When compared with the 1st trajectory cluster, no significant change of the sub-micrometer THNS mass concentration was observed. One possible cause of the less pronounced super-micrometer mass fraction is the efficient wet deposition through drizzle commonly caused by fogs, thought to be dominating in the marginal ice zone, as relatively warm moist air is advected in over the pack ice, while being saturated by cooling from the surface (Heintzenberg et al., 2006, 2012; Nilsson and Leck, 2002). However, such conditions could equally have applied

ACPD
13, 9801–9847, 2013

to the 1st trajectory cluster. Another maybe more relevant cause relates to the reduced synoptic activity encountered, during the 2nd cluster, and expected lower surface wind speeds at the MIZ/open water, which would have resulted in a weaker flux of jet drops with subsequent lower mass apportioned in the super-micrometer size fraction.

To be able to view the distribution in the measured polysaccharide data between R3 and R4 we divided the samples collected within the 4th trajectory cluster into two sub-clusters, Fig. 4a (DOY 240–243) and Fig. 4b (DOY 244–246), respectively. The trajectory sub-clusters are pictured in Fig. 3f, g and represent air that spent ca. 7 days or more over the pack ice. A clear decrease in THNS concentrations is shown in Fig. 6, R3 (cluster 4a) excluded, with increasing length of time spent over the pack ice since last contact with open sea. This is consistent with previous result from samples collected over the central Arctic Ocean by Heintzenberg et al. (2006) and during ASCOS (Heintzenberg and Leck, 2012) based on modal statistics of aerosol concentration by number. Also as referred to above the stronger aerosol flux reported over the open sea compared with those from the open leads (Nilsson et al., 2001; Held et al., 2011a) could serve as an explanation of our measurements.

The comparably high THNS levels in the sub-micrometer size range together with the very low THNS mass fraction in the super-micrometer part of the samples collected during R3 (cluster 4a) needs to be further investigated. The very strong predominance of hexose mass in the Aitken mode, shown in Fig. 7, stands out when comparing the BCI size distributions measured within R3 with the statistics of all samples collected during PI-drift. Fig. 8 shows a comparison of the median relative mass contribution of the monosaccharides determined in the Aitken mode of cluster 4a (Fig. 8a) with the median relative mass contribution to the sub-micrometer aerosol collected during the PI-drift (Fig. 8b). A study of Panagiotopoulos and Sempere (2005) showed that dissolved particulate matter in seawater, from various locations, is distinguishable in terms of their monosaccharide composition. The corresponding relative mass distribution of the nascent aerosol is shown in Fig. 8c, The nascent particles were in situ generated by artificial bubble bursting at the open lead site adjacent to the drifting ice floe and

ACPD
13, 9801–9847, 2013

should therefore be specific for material from the lead surface waters. The higher sub-micrometer mass contribution of glucose + mannose (78 %) collected during DOY 242 (Fig. 8a) relative to what was found both in the nascent particles and in general for the sub-micrometer aerosol collected during PI-drift, Fig. 8b, (41 % on average), indicated that the air masses sampled onboard ship had likely been in contact with continental combustion sources (Carvalho et al., 2003; Tominaga et al., 2011). Based on the hexose fingerprint we speculate that the surface air that mixed with the upper part of the boundary layer (discussed in Sect. 4.2) was influenced by continental sources. In a parallel study performed during ASCOS, Chang et al. (2011) lend strong support to the air originating from continental combustion sources, since elevated levels of acetonitrile (combustion of biomass) and ^{210}Pb (a continental tracer) were observed.

6.2 Changes since last time in contact with open sea

It has become clear from the above discussion, that understanding chemical transformations over the pack ice, that will shape the observed particle polysaccharide mass size distributions at the location of the ship, will also require an understanding of the synoptic scale systems advecting heat, moisture, and particles from the surrounding open seas for a variable length of time over the pack ice. In Fig. 9 we have utilized the travel time over ice since last contact with open sea, DOI, as a simple parameter to summarize the evolution of the airborne particulate polysaccharide, with the sugar composition divided into three categories (THNS, structural or cellular materials of phytoplankton, pentose and hexose, and extracellular deoxysugars). Close to the ice edge and after travel times up to two days, a decline region is indicated for the apportioned polysaccharide mass in the sub-micrometer size range (Aitken-and accumulation modes). Concentration minima for two of the three categories occurs for $2 \leq \mathrm{DOI} < 4$ days beyond which all three increase in the sub-micrometer size range again further into the ice. The extracellular deoxysugars started to incraese already after 3 DOI. For the longest travel times both the structural and extracellular sugars dominates the sub-micrometer size range (close to 90 %).

ACPD
13, 9801–9847, 2013

Based on statistics of modal aerosol number concentrations (Heintzenberg and Leck, 2012) the travel-time dependencies including data from four subsequent expeditions, to the same area and season during 1991 (Leck et al., 1996), 1996 (Leck et al., 2001), 2001 (Leck et al., 2004; Tjernström et al., 2004) and 2008, showed a sink region for DOI < 2 days for particles in the sub-micrometer sizes range and indicated particle sources in the inner Arctic being most pronounced in sizes below 26 nm in diameter. Based on the results of other analyses this has been suggested before (Kerminen and Leck, 2001; Leck and Bigg, 1999, 2005a,b, 2010; Leck et al., 2002). However, overall the direct particle number fluxes determined by the Held et al. (2011a,b) showed that the direct contribution of the open lead particle emissions to the atmospheric aerosol number concentration could only explain a few percent of the observed total particle number variability measured onboard the ship. Unfortunately, no information about the size of the emitted particles was available from these direct flux measurements so a direct comparison with different particle modes cannot be done.

6.3 The relevance of polysaccharides for cloud activation

What past studies also have shown is a potential for the airborne polymer gels, with their partially colloidal (extracellular) and granular (structural) structures (Leck and Bigg, 2005a, 2010; Orellana et al., 2011), to separate into colloidal fragments having sizes within the sub accumulation mode peaking in the Aitken mode around 40 nm in diameter. More than 80 % of the gel particles were detected smaller than 100 nm in diameter, and nearly 100 % were smaller than 200 nm. Polymer gels in sizes as small as 2 nm in diameter could be quantified. The fragmentation process would be promoted with exposure of ultraviolet light (Orellana et al., 2011) and long travel times over the pack ice. In an attempt to explain the characteristics of fragmentation of polymer gels in the high Arctic a hypothesis has been put forward linking the it to evaporation of cloud – or fog droplets by mixing with dry air at the top and edges of a cloud/fog (Leck and Bigg, 1999, 2010), whereby particle breakup could take place during evaporation. The presence of a fragmentation mechanism could also serve as a model to explain why

ACPD
13, 9801–9847, 2013

only a few percent of the observed total particle number variability measured onboard the ship was explained by the direct eddy covariance measurements of particle number fluxes at the open lead site, however it needs further elaboration.

Moreover, the relatively high abundance of extracellular deoxysugars in the Aitken mode in air being advected over the pack ice is indicative of the presence of highly surface-active constituents (Gao et al., 2012). The Aitken mode particles, observed in this study, associated with the microgels found in the open lead surface microlayer (Gao et al., 2012) could thus be important for cloud droplet formation over the inner summer Arctic. Those findings are in agreement with the recent study by Orrelana et al. (2011) that strongly advocated that the marine microgels dominate the available CCN number population in the high Arctic (north of 80° N) during the summer season.

7 Conclusions

The novelty of using the LC/MS/MS technique provided the first time detection of marine biogenic polysaccharides in airborne aerosols resolved over size. The samples for determination were collected over the central Arctic perennial ice during the biologically most active period between the late summer melt season and into the transition to autumn freeze-up. The size-resolved data of the monosaccharides in combined form (polysaccharides) showed a distinctive feature of heteropolysaccharides, enriched in the pentose xylose, hexoses glucose + mannose as well as a substantial fraction of deoxysugars (rhamnose and fucose).

From 3 August to 8 September 2008, THNS mass concentration within the supermicrometer particle size range varied over 3 orders of magnitude (1–692 pmol m^{-3}) and to a lesser extent in the sub-micrometer particles (4–88 pmol m^{-3}). The highest THNS values were observed in the open waters and along the ice edge zone of the Greenland Sea–Fram Strait area, in August. In September both the OW and MIZ concentrations had declined by about 45 %. For all monosaccharides investigated the lowest concentrations were found in air masses that had spent more than 5 days over the pack ice

ACPD
13, 9801–9847, 2013

area since last contact with open sea. The results could be explained by the more biologically active waters of the Greensand Sea–Fram Strait area and the much stronger flux of bubble bursting aerosol over the open sea than from open leads. For samples collected during the PI-drift on average 53 ± 24 % of the THNS was apportioned in the Aitken and accumulation mode, increasing to more than 90 % with a longer length period of time (DOI > 7 days) spent over the pack ice.

The mass size distributions of extracellular deoxysugars exhibited a clear bimodal structure with peak concentrations in the Aitken mode both in samples collected during the PI-drift and during the MIZ/OW stations whereas the structural sugars, pentose and hexose, showed a less pronounced bimodal character with peak concentrations frequently associated with the course mode.

The dependence of polysaccharide mass size distribution on the air mass residence time over the pack ice, especially pronounced for the sub-micrometer particles, is indicative of particle sources in the inner Arctic. The similarity in monosaccharide fingerprint between the ambient aerosol and those in situ generated at the open lead site lends support to the suggestion that bubble bursting is capable of providing the Aitken particles originating from marine polymer microgels. However, overall the direct particle number fluxes carried out by the Held et al. (2011a,b) found that the direct contribution of the open lead particle emissions to the atmospheric aerosol number concentration could only explain a few percent of the observed total particle number variability measured onboard the ship. We speculate that there is a potential for the polymer gels, with their partially colloidal (extracellular) and granular (structural) structures and with time spent in the air, to separate into colloidal fragments after exposure to ultraviolet light (Orellana et al., 2011) and subsequent disruption of particles as been suggested by Leck and Bigg (1999, 2010). The presence of such a fragmentation mechanism could also serve as a model to explain the discrepancy between the observed total particle number variability measured onboard the ship.

The occurrence of surface-active and hygroscopic polysaccharides in airborne particles, as demonstrated in this study, suggests that polymer microgels could potentially

ACPD
13, 9801–9847, 2013

become important for cloud droplet activation over the inner summer Arctic. It is hoped that this possibility (whether it turns out to be significant or not) will renew interest in the complex but fascinating interactions between marine microbiology, aerosol, clouds and climate.

Acknowledgements. We thank Linda Orr for providing the back trajectories. Matthias Karl's comments on an early version of the article are appreciated. This work is part of ASCOS (the Arctic Summer Cloud Ocean Study). ASCOS was made possible by funding from the Knut and Alice Wallenberg Foundation and the DAMOCLES European Union 6th Framework Program Integrated Research Project. The Swedish Polar Research Secretariat (SPRS) provided access to the icebreaker *Oden* and logistical support. Michael Tjernström are specifically thanked for his co-coordination of ASCOS. We are grateful to the SPRS logistical staff and to *Oden*'s Captain Mattias Peterson and his crew. ASCOS is an IPY project under the AICIA-IPY umbrella and an endorsed SOLAS project. Support for this work was provided by the Swedish Research Council (VR) and the Knut and Alice Wallenberg Foundation.

References

Berner, A., Luzer, C., Pohl, F., Preining, O., and Wagner, P.: The size distribution of the urban aerosol in Vienna, Sci. Total Environ., 13, 245–261, 1979.

Bigg, E. K.: Comparison of aerosol at four baseline atmospheric monitoring stations, J. Appl. Meteorol., 19, 521–533, 1980.

Bigg, E. K.: Sources, nature and influence on climate of marine airborne particles, Environ. Chem., 4, 155–161, 2007.

Bigg, E. K. and Leck, C.: Cloud-active particles over the central Arctic Ocean, J. Geophys. Res., 106, 32155–32166, 2001.

Bigg, E. K. and Leck, C.: The composition of fragments of bubbles bursting at the ocean surface, J. Geophys. Res., 113, D11209, doi:10.1029/2007JD009078, 2008.

Bigg, E. K., Leck, C., and Nilsson, E. D.: Sudden changes in arctic atmospheric aerosol concentrations during summer andautumn, Tellus B, 48, 254–271, 1996.

ACPD
13, 9801–9847, 2013

Bigg, E. K., Leck, C., and Nilsson, E. D.: Sudden changes in aerosol and gas concentrations in the central Arctic marine boundary layer: causes and consequences, J. Geophys. Res., 106, 32167–32185, 2001.
Bigg, E. K., Leck, C., and Tranvik, T.: Particulates of the surface microlayer of open water in the central Arctic Ocean in summer, Mar. Chem., 91, 131–141, 2004.
Blanchard, D. C.: The Oceanic Production of Volatile Cloud Nuclei, J. Atmos. Sci., 28, 811–812, 1971.
Blanchard, D. C. and Syzdek, L. D.: Film drop production as a function of bubble size, J. Geophys. Res., 93, 3649–3654, 1988.
Carvalho, A., Pio, C., and Santos, C.: Water-soluble hydroxylated organic compounds in German and Finnish aerosols, Atmos. Environ., 37, 1775–1783, 2003.
Chang, R. Y.-W., Leck, C., Graus, M., Müller, M., Paatero, J., Burkhart, J. F., Stohl, A., Orr, L. H., Hayden, K., Li, S.-M., Hansel, A., Tjernström, M., Leaitch, W. R., and Abbatt, J. P. D.: Aerosol composition and sources in the central Arctic Ocean during ASCOS, Atmos. Chem. Phys., 11, 10619–10636, doi:10.5194/acp-11-10619-2011, 2011.
Chin, W.-C., Orellana, M. V., and Verdugo, P.: Spontaneous assembly of marine dissolved organic matter into polymer gels, Nature, 391, 568–572, 1998.
Decho, A. W.: Microbial exopolymer secretions in ocean environments: their role(s) in food webs and marine processes, Oceanogr. Mar. Biol. Ann. Rev., 28, 73–153, 1990.
Draxler, R. R. and Rolph, G. D.: HYSPLIT (HYbrid Single-Particle Lagrangian Integrated Trajectory) Model access via NOAA ARL READY Website, available at: http://ready.arl.noaa.gov/HYSPLIT.php, NOAA Air Resources Laboratory, Silver Spring, MD, 2011.
English, T. S.: Some biological oceanograph observations in the central North Polar Sea, Sc. Rpt. 15, Res. Paper 13, Arctic Inst. North America, Calgary, 79 pp., 1961.
Facchini, M. C., Rinaldi, M., Decesari, S., Carbone, C., Finessi, E., Mircea, M., Fuzzi, S., Ceburnis, D., Flanagan, R., Nilsson, E. D., de Leeuw, G., Martino, M., Woeltjen, J., and O'Dowd, C. D.: Primary submicron marine aerosol dominated by insoluble organic colloids and aggregates, Geophys. Res. Lett., 35, L17814, doi:10.1029/2008GL034210, 2008.
Gao, Q., Araia, M., Leck, C., and Emmer, A.: Characterization of exopolysaccharides in marine colloids by capillary electrophoresis with indirect UV detection, Anal. Chim. Acta, 662, 193–199, 2010.

ACPD
13, 9801–9847, 2013

Gao, Q., Nilsson, U., Ilag, L. L., and Leck, C.: Monosaccharide compositional analysis of marine polysaccharides by hydrophilic interaction liquid chromatography-tandem mass spectrometry, Anal. Bioanal. Chem., 399, 2517–2529, 2011.

Gao, Q., Leck, C., Rauschenberg, C., and Matrai, P. A.: On the chemical dynamics of extracellular polysaccharides in the high Arctic surface microlayer, Ocean Sci., 8, 401–418, doi:10.5194/os-8-401-2012, 2012.

Giroldo, D., Vieira, A., and Paulsen, B.: Relative increase of deoxy sugars during microbial degradation of an extracellular polysaccharide released by a tropical freshwater *Thalassiosira SP*, J. Phycol., 39, 1109–1115, 2003.

Gras, J. L. and G. P. Ayers, Marine aerosol at southern midlatitudes, J. Geophys. Res., 88, 10661–10666, 1983.

Hansell, D. A. and Carlson, C. A.: Biogeochemistry of Marine Dissolved Organic Matter, Academic Press, San Diego, 2002.

Hawkins, L. N. and Russell, L. M.: Polysaccharides, Proteins, and Phytoplankton Fragments: Four Chemically Distinct Types of Marine Primary Organic Aerosol Classified by Single Particle Spectromicroscopy, Advances in Meteorology, 2010, 612132, doi:10.1155/2010/612132, 2010.

Heintzenberg, J. and Leck, C.: The summer aerosol in the central Arctic 1991–2008: did it change or not?, Atmos. Chem. Phys., 12, 3969–3983, doi:10.5194/acp-12-3969-2012, 2012.

Heintzenberg, J., Leck, C., Birmili, W., Wehner, B., Tjernström, M., and Wiedensohler, A.: Aerosol number-size distributions during clear and fog periods in the summer high Arctic: 1991, 1996 and 2001, Tellus B, 58, 41–50, 2006.

Held, A., Brooks, I. M., Leck, C., and Tjernström, M.: On the potential contribution of open lead particle emissions to the central Arctic aerosol concentration, Atmos. Chem. Phys., 11, 3093–3105, doi:10.5194/acp-11-3093-2011, 2011.

Held, A., Orsini, D. A., Vaattovaara, P., Tjernström, M., and Leck, C.: Near-surface profiles of aerosol number concentration and temperature over the Arctic Ocean, Atmos. Meas. Tech., 4, 1603–1616, doi:10.5194/amt-4-1603-2011, 2011.

Intrieri, J. M., Shupe, M. D., Uttal, T., and McCarty, B. J.: An annual cycle of Arctic cloud characteristics observed by radar and lidar at SHEBA, J. Geophys. Res., 107, 8030, doi:10.1029/2000JC000423, 2002.

IUPAC, Analytical Chemistry Division: Nomenclature, symbol, units and their usage inspectrochemical analysis – II. Data interpretation, Spectrochim. Acta B, 33, 241–246, 1978.

ACPD
13, 9801–9847, 2013

IPCC, Climate Change 2007: The Physical Science Basis, Contribution of Working Group I to the Fourth Assesment Report of the Intergovernmental Panel on Climate Change. Cambridge University Press, Cambridge, 2007.
Karlsson, J. and Svensson, G.: The simulation of Arctic clouds and their influence on the winter surface temperature in present-day climate in the CMIP3 multi-model dataset, Clim. Dynam., 36, 623–635, 2011.
Kerminen, V.-M. and Leck, C.: Sulfur chemistry over the central Arctic Ocean during the summer: gas-to-particle transformation, J. Geophys. Res., 106, 32087–32099, 2001.
Kuznetsova, M., Lee, C., and Aller, J.: Characterization of the proteinaceous matter in marine aerosols, Mar. Chem., 96, 359–377, 2005.
Leck, C. and Bigg, E. K.: Aerosol production over remote marine areas – a new route, Geophys. Res. Lett., 23, 3577–3581, 1999.
Leck, C. and Bigg, E. K.: Evolution of the marine aerosol – a new perspective, Geophys. Res. Lett., 32, L19803, doi:10.1029/2005GL023651, 2005a.
Leck, C. and Bigg, E. K.: Biogenic particles in the surface microlayer and overlaying atmosphere in the central Arctic Ocean during summer, Tellus B, 57, 305–316, 2005b.
Leck, C. and Bigg, E. K.: Comparison of sources and nature of the tropical aerosol with the summer high Arctic aerosol, Tellus B, 60, 118–126, doi:10.1111/j.1600-0889.2007.00315.x, 2008.
Leck, C. and Bigg, E. K.: New particle formation of marine biological origin, Aerosol Sci. Technol., 44, 570–577, 2010.
Leck, C. and Persson, C.: Seasonal andshort-term variability in dimethyl sulfide, sulfur dioxide and biogenic sulfurand sea salt aerosol particles in the arctic marine boundary layer, during summer and autumn, Tellus B, 48, 272–299, 1996a.
Leck, C. and Persson, C.: The central Arctic Ocean as a source of dimethyl sulfide: seasonal variability in relation to biological activity, Tellus B, 48, 156–177, 1996b.
Leck, C., Bigg, E. K., Covert, D. S., Heintzenberg, J., Maenhaut, W., Nilsson, E. D., and Wiedensohler, A.: Overview of the atmospheric research program during the International Arctic Ocean Expedition of 1991 (IAOE-91) and its scientific results, Tellus B, 48, 136–155, 1996.
Leck, C., Nilsson, E. D., Bigg, E. K., and Bäcklin, L.: Atmospheric program on the Arctic Ocean Expedition 1996 (AOE-96): an overview of scientific goals, experimental approaches, and instruments, J. Geophys. Res., 106, 32051–32067, 2001.

ACPD
13, 9801–9847, 2013

Leck, C., Norman, M., Bigg, E. K., and Hillamo, R.: Chemical composition and sources of the high Arctic aerosol relevant for cloud formation, J. Geophys. Res., 107, 4135, doi:10.1029/2001JD001463, 2002.
Leck, C., Tjernström, M., Swietlicki, E., and Bigg, E. K.: Can marine micro-organisms influence melting of the Arctic pack ice?, EOST. Am. Geophys. Un., 85, 25–36, 2004.
Lia, B. Y. H. and Lee, K. W.: Efficiency of membrane and Nuclepore filters for sub-micrometer aerosols, Environ. Sci. Technol., 10, 345–350, 1976.
Matrai, P. A., Tranvik, L., Leck, C., and Knulst, J. C.: Are high Arctic surface microlayers a potential source of aerosol organic precursors?, Mar. Chem., 108, 109–122, 2008.
Mauritsen, T., Sedlar, J., Tjernström, M., Leck, C., Martin, M., Shupe, M., Sjogren, S., Sierau, B., Persson, P. O. G., Brooks, I. M., and Swietlicki, E.: An Arctic CCN-limited cloud-aerosol regime, Atmos. Chem. Phys., 11, 165–173, doi:10.5194/acp-11-165-2011, 2011.
Mopper, K., Zhou, J., Sri Ramana, K., passow, U., dam, H. G., and Drapeau, D. T.: The role of surface-active carbohydrates in the flocculation of a diatom bloom in a mesocosm, Deep-Sea Res. Pt. II, 42, 47–73, 1995.
Nilsson, E. D.: Planetary boundary layer structure and air mass transport during the International Arctic Ocean Expedition 1991, Tellus B, 48, 178–196, 1996.
Nilsson, E. D. and Bigg, E. K.: Influences on formation and dissipation of high arctic fogs during summer and autumn and their interaction with aerosol, Tellus B, 48, 234–253, 1996.
Nilsson, E. D., Rannik, Ü., Swietlicki, E., Leck, C., Aalto, P. P., Norman, M., and Zhou, J.: Turbulent aerosol number fluxes during theArctic Ocean Expedition 1996 – Part II: A wind driven source of sub micrometeraerosol particles from the sea, J.Geophys. Res., 106, 32,139–32,154, 2001.
Nilsson, E. D. and Leck, C.: A pseudo-Lagrangian study of the sulfur budget in the remote Arctic marine boundary layer, Tellus B, 54, 213–230, 2002.
Norris, S. J., Brooks, I. M., de Leeuw, G., Sirevaag, A., Leck, C., Brooks, B. J., Birch, C. E., and Tjernström, M.: Measurements of bubble size spectra within leads in the Arctic summer pack ice, Ocean Sci., 7, 129–139, doi:10.5194/os-7-129-2011, 2011.
O'Dowd, C. D., Lowe, J. A., Smith, M. H., and Kaye, A. D.: The relative importance of non-sea-salt sulphate and sea-salt aerosol to the marine cloud condensation nuclei population: an improved multi-component aerosol-cloud droplet parameterization, Q. J. Roy. Meteor. Soc., 125, 1295–1313, 1999.

ACPD
13, 9801–9847, 2013

Ogren, J. A. and Heintzenberg, J.: Parametric Aerosol Sampling at Low Concentration Levels, Rap. AA-1, Department of Meteorology, Stockholm University, 1990.
Olli, K., Wassmann, P., Reigstad, M., Ratkova, T. N., Arashkevich, E., Pasternak, A., Matrai, P. A., Knulst, J., Tranvik, L., Klais, R., and Jacobsen, A.: The fate of production in the central Artic Ocean – top-down regulation by zooplankton expatriates? Results from a 3 week ice drift at 88° N, Prog. Oceanogr., 72, 84–113, 2007.
Orellana, M. V., Matrai, P. A., Leck, C., Rauschenberg, C. D., Lee, A. M., and Coz, E.: Marine microgels as a source of cloud condensation nuclei in the high Arctic, Proc. Natl. Acad. Soc. USA, 108, 13612–13617,2011.
Paatero, J., Vaattovaara, P., Vestenius, M., Meinander, O., Makkonen, U., Kivi, R., Hyvärinen, A., Asmi, E., Tjernström, M., and Leck, C.: Finnish contribution to the Arctic Summer Cloud Ocean Study (ASCOS) expedition, Arctic Ocean 2008, Geophysica, 45, 119–146, 2009.
Panagiotopoulos, C. and Sempere, R.: The molecular distribution of combined aldoses in sinking particles in various oceanic conditions, Mar. Chem., 95, 31–49, 2005.
Posfai, M., Simonics, R., Li, J., Hobbs, P. V., and Buseck, P. R.: Individual aerosol particles from biomass burning in southern Africa: 1. Compositions and size distributions of carbonaceous particles, J. Geophys. Res., 108, 8483, doi:10.1029/2002JD002291, 2003.
Rolph, G. D.: Real-time Environmental Applications and Display sYstem (READY) Website, available at: http://ready.arl.noaa.gov, NOAA Air Resources Laboratory, Silver Spring, MD, 2011.
Russell, L. M., Hawkins, L. N., Frossard, A. A., Quinn, P. K., and Bates, T. S.: Carbohydrate like composition of submicron atmospheric particles and their production from ocean bubble bursting, P. Natl. Acad. Sci. USA, 107, 6652–6657, doi:10.1073/pnas.0908905107, 2010.
Sedlar, J., Tjernström, M., Mauritsen, T., Shupe, M. D., Brooks, I. M., Persson, P. O. G., Birch, C. E., Leck, C., Sirevaag, A., and Nicolaus, M.: A transitioning Arctic surface energy budget: the impacts of solar zenith angle, surface albedo and cloud radiative forcing, Clim. Dynam., 37, 1643–1660, doi:10.1007/s00382-010-0937-5, 2010.
Sirevaag, A., de la Rosa, S., Fer, I., Nicolaus, M., Tjernström, M., and McPhee, M. G.: Mixing, heat fluxes and heat content evolution of the Arctic Ocean mixed layer, Ocean Sci., 7, 335-349, doi:10.5194/os-7-335-2011, 2011.
Skoog, A. and Benner, R.: Aldoses in various size fractions of marine organic matter: implications for carbon cycling, Limnol. Oceanogr., 42, 1803–1813, 1998.

ACPD
13, 9801–9847, 2013

Smith, W. O. and Nelson, D. M.: Phytoplankton bloom produced by a receding ice edge in the ross sea: spatial coherence with the density field, Science, 227, 163–166, 1985.
Tjernström, M.: The summer Arctic boundary layer during the Arctic Ocean Experiment 2001 (AOE-2001), Bound.-Lay. Meteorol., 117, 5–36, 2005.
Tjernström, M., Sedlar, J., and Shupe, M. D.: How well do regional climate models reproduce radiation and clouds in the arctic? An evaluation of ARCMIP simulations, J. Appl. Meteorol., 47, 2405–2422, 2008.
Tjernström, M., Birch, C. E., Brooks, I. M., Shupe, M. D., Persson, P. O. G., Sedlar, J., Mauritsen, T., Leck, C., Paatero, J., Szczodrak, M., and Wheeler, C. R.: Meteorological conditions in the central Arctic summer during the Arctic Summer Cloud Ocean Study (ASCOS), Atmos. Chem. Phys., 12, 6863-6889, doi:10.5194/acp-12-6863-2012, 2012.
Tjernström, M., Leck, C., Birch, C. E., Bottenheim, J. W., Brooks, B. J., Brooks, I. M., Bäcklin, L., Chang, R. Y.-W., Granath, E., Graus, M., Hansel, A., Heintzenberg, J., Held, Hind, A., de la Rosa, S., Johnston, P., Knulst, J., de Leuuw, G., di Liberto, L., Martin, M., Matrai, P. A., Mauritsen, T., Müller, M., Norris, S. J., Orellana, M. V., Orsini, D. A., Paatero, J., Persson, P. O. G., Gao, Q., Rauschenberg, C., Ristovski, Z., Sedlar, J., Shupe, M. D., Sireau, B., Sirevaag, A., Sjogren, S., Stetzer, O., Swietlicki, E., Szczodrak, M., Vaattovaara, P., Wahlberg, N., Westberg, M., and Wheeler, C. R.: The Arctic Summer Cloud-Ocean Study (ASCOS): overview and experimental design, Atmos. Chem. Phys. Discuss., in review, 2013.
Tominaga, S., Matsumoto, K., Kaneyasu, N., Shigihara, A., Katono, K., and Igawa, M.: Measurements of particulate sugars at urban and forested suburban sites, Atmos. Environ., 45, 2335–2339, 2011.
Verdugo, P.: Marine microgels, Ann. Rev. Mar. Sci., 4, 375–400, 2012.
Walsh, J. E., Kattsov, V. M., Chapman, W. L., Govorkova, V., and Pavlova, T.: Comparison of Arctic climate simulations by uncoupled and coupled global models, J. Clim., 15, 1429–1446, 2002.
Wedyan, M. A. and Preston, M. R.: The coupling of surface seawater organic nitrogen and the marine aerosol as inferred from enantiomer-specific amino acid analysis, Atmos. Environ., 42, 8698–8705, 2008.
Widell, B.: Development of GC-HRMS Procedures for Determination of Naturally Occuring Polar Compounds in Various Environmental Applications, Doctoral Thesis, Department of Applied Environmental Science (ITM), Stockholm Universiy, Stockholm, 2009.

ACPD
13, 9801–9847, 2013

Zhou, J., Mopper, K., and Passow, U.: The role of surface-active carbohydrates in the formation of transparent exopolymer particles by bubble adsorption of seawater, Limnol. Oceanogr., 43, 1860–1871, 1998.

ACPD
13, 9801–9847, 2013

Table 1. Accuracy, precision (% RSD), limits of detection (LOD) and limits of quantification (LOQ) of the analytes determined.

Analytes	Method LOD ($pmol\,m^{-3}$)	Method LOQ ($pmol\,m^{-3}$)	RSD ($n = 6$)	Accuracy, % 40 $ng\,mL^{-1}$	200 $ng\,mL^{-1}$
Xylose	0.05	0.16	14.5	105.0	90.7
Arabinose	0.08	0.28	9.0	86.8	105.9
Rhamnose	0.04	0.13	21.2	87.3	108.6
Fucose	0.07	0.22	15.7	96.4	109.1
Glucose + Mannose	0.05	0.15	19.3	84.4	90.0
Galactose	0.05	0.18	13.7	78.0	89.1

ACPD
13, 9801–9847, 2013

Table 2. Monosaccharide composition of size-resolved aerosol particles collected during AS-COS.

Station	Sampling period in DOY (No. of samples)	Size range[a]	THNS, pmol m^{-3}	% Sub to the mass of total	Monosaccharide composition, %					
					Xylose	Arabinose	Rhamnose	Fucose	Glucose + Mannose	Galactose
OW1	216.561–217.342 (1)	Sub	88.3	39.2	36.9	2.9	8.0	2.0	36.3	13.9
		Super	137.0		25.3	6.3	33.4	n.d.[b]	20.2	14.9
MIZ1	217.503–218.508 (1)	Sub	73.0	38.6	55.2	2.3	8.7	n.d.	26.6	7.2
		Super	116.0		33.0	2.4	0.3	1.3	56.5	6.4
PI-drift	225.967–245.952 (14)	Sub Median	24.8	50 (34.0, 69.6)[e]	32.0	3.8	10.8	0.4	47.1	6.3
		25th percentile	11.7		17.1	2.3	6.1	0.1	33.4	3.1
		75th percentile	26.9		36.8	5.2	23.3	2.0	56.3	8.3
		Super Median	12.7		28.0	1.2	3.3	1.6	52.5	7.8
		25th percentile	7.3		22.6	n.d.	1.4	0.2	32.8	1.7
		5th percentile	28.7		39.4	3.2	4.5	4.2	63.9	12.9
		% D.F.[d]	–		82.9	55.7	45.7	42.9	92.8	60.1
MIZ2	250.468–251.091 (1)	Sub	81.6	73.4	49.4	n.d.	7.0	n.d.	36.4	7.2
		Super	29.6		599.9	3.7	5.6	n.d.	28.4	2.3
OW2	251.181–251.666 (1)	Sub	84.8	65.8	35.7	1.9	24.3	n.d.	38.2	n.d.
		Super	44.1		18.2	1.7	2.4	n.d.	63.6	n.d.

[a] Particles in the (Sub)-micrometer size range (sum of BCI stage 1 and 2) and (Super)-micrometer size range (sum of BCI stage 3, 4 and 5).
[b] n.d. = The value is below detection limit.
[c] The values indicated in the parenthesis represent 25th and 75th percentile value of the % Sub- to THNS.
[d] % D.F. = % detection freque

ACPD
13, 9801–9847, 2013

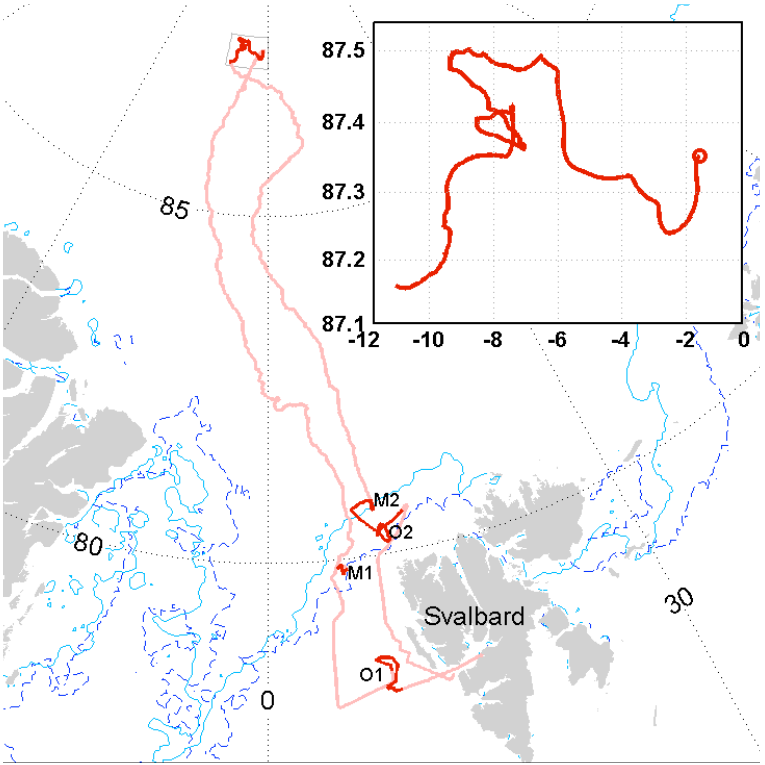

Fig. 1. Map of the ASCOS cruise track (pink) with ice-drift period (PI-drift) highlighted (red) and (inset) shown in detail with the start of the drift marked by the circle. The left-hand part of the track shows the initial northward track while the right-hand track shows the southward, return track. Convoluted track lines in open water, OW (O1 and O2) and at the ice edge, MIZ (M1 and M2) are associated with shorter sampling stations. The ice edge (blue line) is shown for the start of the drift period on 12 August 2008.

ACPD
13, 9801–9847, 2013

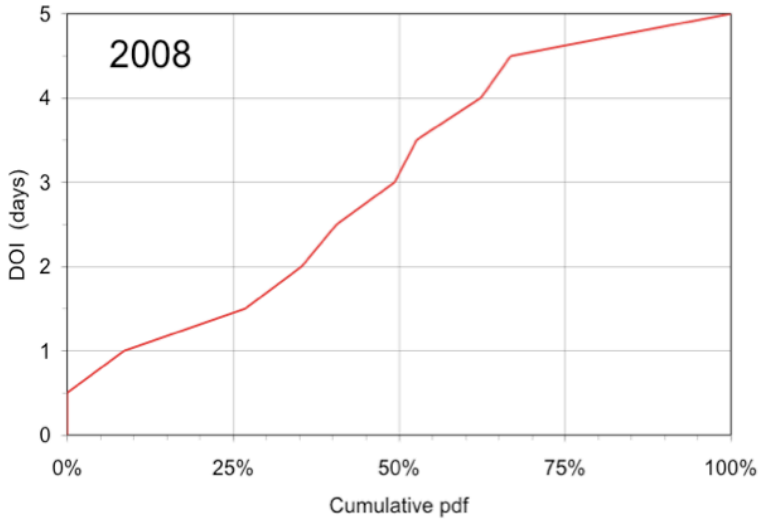

Fig. 2. Cumulative probability distributions of travel times over ice (DOI, days) for the icebreaker *Oden* during ASCOS 2008. Travel times beyond five days are given the value five.

ACPD
13, 9801–9847, 2013

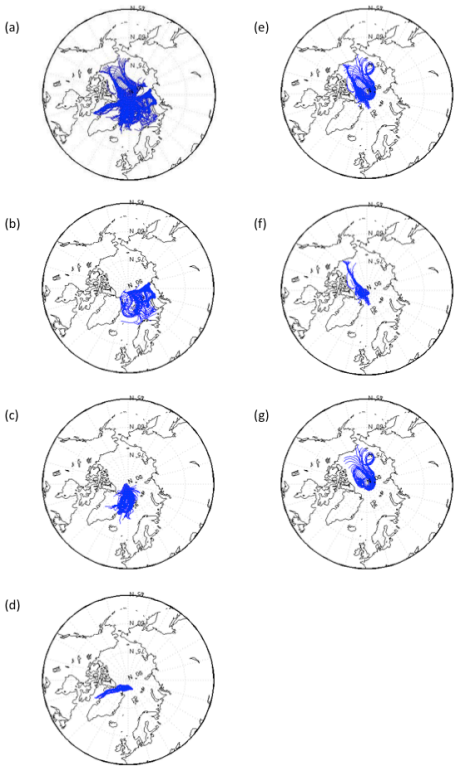

Fig. 3. Air mass trajectory clusters with an arrival height of 100 m at the position of the ice-breaker during: **(a)** the ice drift (PI-drift), **(b)** cluster 1 (DOY 227, DOY 229–232) originated easterly from the Barents- and Kara Seas, **(c)** cluster 2 (DOY 228, DOY 236, 238–239) from the Greenland Sea–Fram Strait area, **(d)** cluster 3 (DOY 234–235) from Greenland, **(e)** cluster 4 (DOY 240–246) from northwestern circumpolar over the pack ice, **(f)** sub-cluster 4a (DOY 240–243), and **(g)** sub-cluster 4b (DOY 243–246).

ACPD
13, 9801–9847, 2013

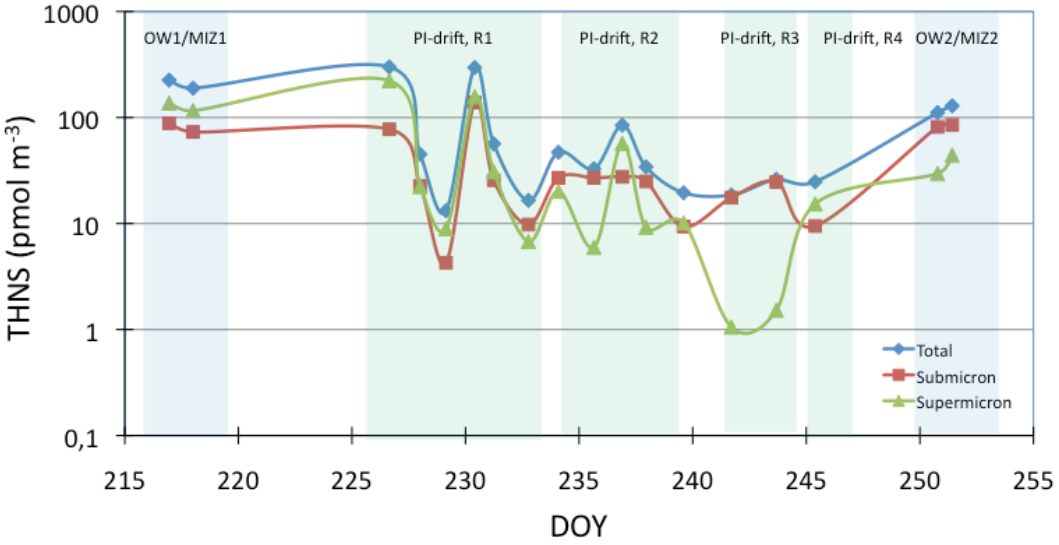

Fig. 4. Temporal variation of particulate THNS mass concentration (pmol m^{-3}), grouped in the sub- and super-micrometer size ranges. The division into four separate regimes (R1–4) during ice drift (PI-drift), based on the analyses of the surface energy budget (see Sect. 4.1 for details), is indicated by light green panels. The inward and outward OW and MIZ stations are indicated by light blue panels.

ACPD
13, 9801–9847, 2013

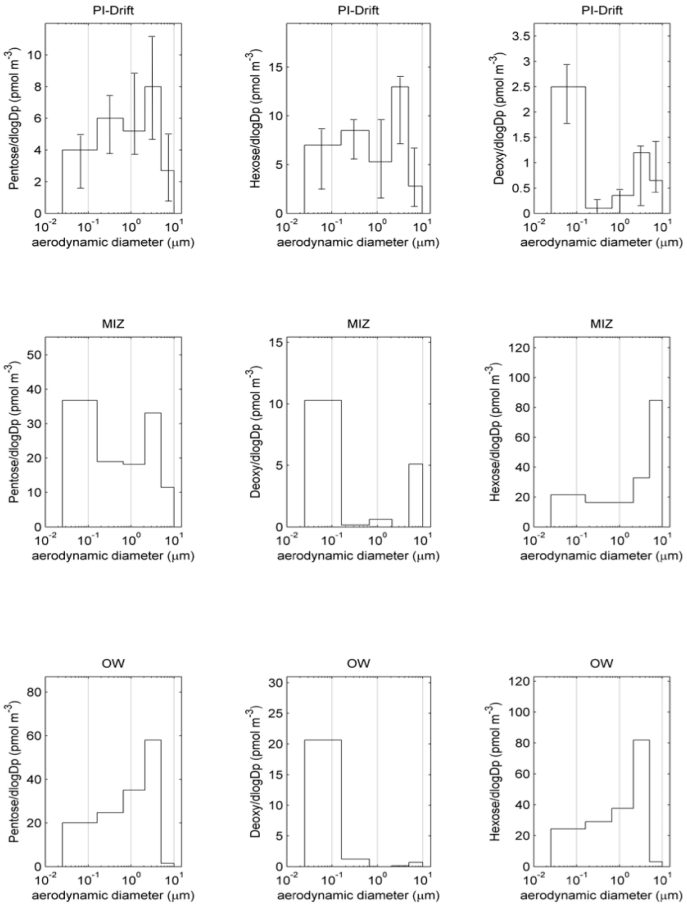

Fig. 5. Size distribution of particulate pentose, hexose and deoxysugars collected (upper panel) over the pack ice during the PI-drift, (middle panel) at the MIZ, and (lower panel) in the OW. Error bars indicate the 25th and 75th percentile values.

ACPD
13, 9801–9847, 2013

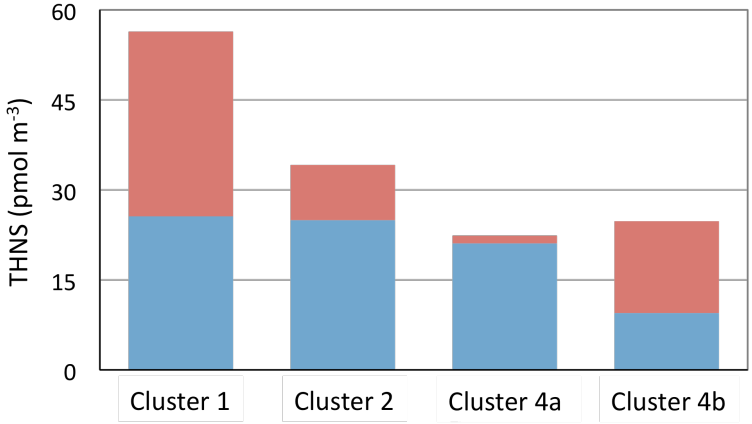

Fig. 6. Median THNS mass concentrations (pmol m^{-3}) of particles in the submicron (blue) and supermicron (red) size ranges, calculated for in trajectory cluster 1, 2, 4a and 4b, respectively.

ACPD
13, 9801–9847, 2013

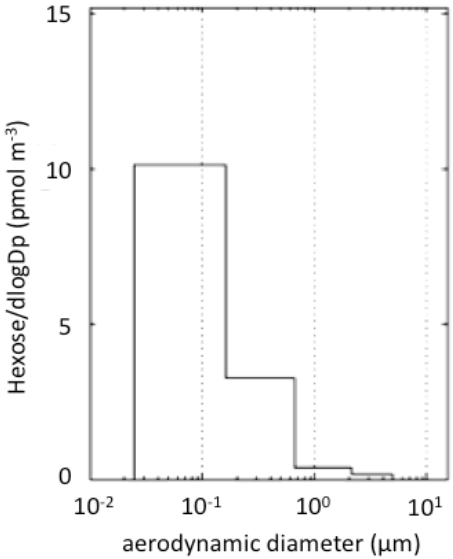

Fig. 7. Mass size distribution of particulate hexose for trajectory cluster 4a during R3.

ACPD
13, 9801–9847, 2013

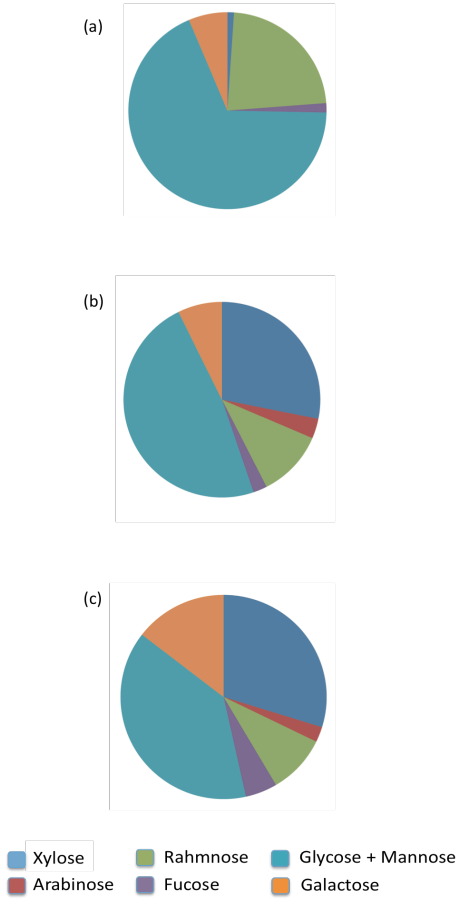

Fig. 8. Relative percentage of monosaccharides determined: **(a)** in the Aitken mode (BCI stage 1) during DOY 242, **(b)** during the PI-drift (Aitken- and accumulation mode), and **(c)** from bubble generated sea spray aerosol at open lead site.

ACPD
13, 9801–9847, 2013

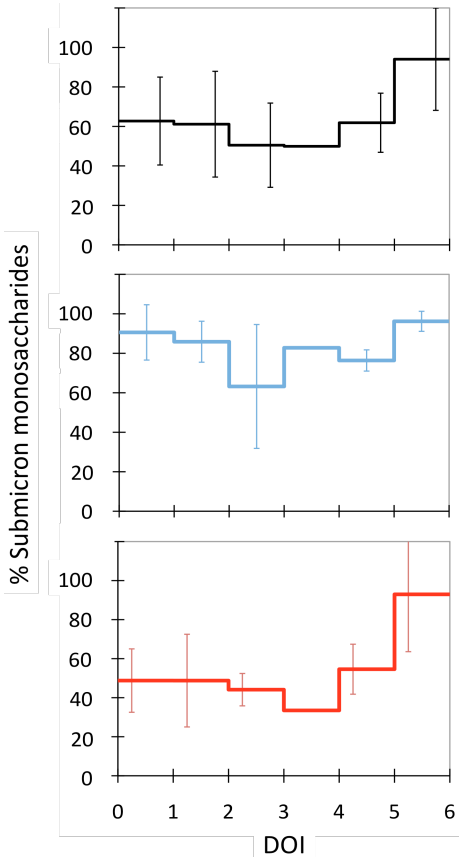

Fig. 9. Relative submicron (Aitken and accumulation mode) to total mass (%), of THNS (dark grey), deoxysugars (light blue) and the sum of pentose and hexose (red) as a function of travel time over ice (DOI). Data for all travel times of five days and longer have been collected in the column 5–6 days. Error bars indicate $\pm 1\sigma$. For $3 < \mathrm{DOI} < 4$ $n = 1$.

ACPD
13, 9801–9847, 2013